

**Evolution of the differential transverse momentum correlation function with centrality  
in Au+Au collisions at  $\sqrt{s_{NN}} = 200$  GeV**  
(STAR Collaboration)

H. Agakishiev,<sup>1</sup> M. M. Aggarwal,<sup>2</sup> Z. Ahammed,<sup>3</sup> A. V. Alakhverdyants,<sup>1</sup> I. Alekseev,<sup>4</sup> J. Alford,<sup>5</sup> B. D. Anderson,<sup>5</sup>  
C. D. Anson,<sup>6</sup> D. Arkhipkin,<sup>7</sup> G. S. Averichev,<sup>1</sup> J. Balewski,<sup>8</sup> D. R. Beavis,<sup>7</sup> N. K. Behera,<sup>9</sup> R. Bellwied,<sup>10</sup>  
M. J. Betancourt,<sup>8</sup> R. R. Betts,<sup>11</sup> A. Bhasin,<sup>12</sup> A. K. Bhati,<sup>2</sup> H. Bichsel,<sup>13</sup> J. Bielcik,<sup>14</sup> J. Bielcikova,<sup>15</sup> B. Biritz,<sup>16</sup>  
L. C. Bland,<sup>7</sup> I. G. Bordyuzhin,<sup>4</sup> W. Borowski,<sup>17</sup> J. Bouchet,<sup>5</sup> E. Braidot,<sup>18</sup> A. V. Brandin,<sup>19</sup> A. Bridgeman,<sup>20</sup>  
S. G. Brovko,<sup>21</sup> E. Bruna,<sup>22</sup> S. Bueltmann,<sup>23</sup> I. Bunzarov,<sup>1</sup> T. P. Burton,<sup>7</sup> X. Z. Cai,<sup>24</sup> H. Caines,<sup>22</sup>  
M. Calderón de la Barca Sánchez,<sup>21</sup> D. Cebra,<sup>21</sup> R. Cendejas,<sup>16</sup> M. C. Cervantes,<sup>25</sup> Z. Chajecski,<sup>6</sup> P. Chaloupka,<sup>15</sup>  
S. Chattopadhyay,<sup>26</sup> H. F. Chen,<sup>27</sup> J. H. Chen,<sup>24</sup> J. Y. Chen,<sup>28</sup> L. Chen,<sup>28</sup> J. Cheng,<sup>29</sup> M. Cherney,<sup>30</sup>  
A. Chikanian,<sup>22</sup> K. E. Choi,<sup>31</sup> W. Christie,<sup>7</sup> P. Chung,<sup>15</sup> M. J. M. Coddington,<sup>25</sup> R. Corliss,<sup>8</sup> J. G. Cramer,<sup>13</sup>  
H. J. Crawford,<sup>32</sup> A. Davila Leyva,<sup>33</sup> L. C. De Silva,<sup>10</sup> R. R. Debebe,<sup>7</sup> T. G. Dedovich,<sup>1</sup> A. A. Derevschikov,<sup>34</sup>  
R. Derradi de Souza,<sup>35</sup> L. Didenko,<sup>7</sup> P. Djawotho,<sup>25</sup> S. M. Dogra,<sup>12</sup> X. Dong,<sup>3</sup> J. L. Drachenberg,<sup>25</sup> J. E. Draper,<sup>21</sup>  
J. C. Dunlop,<sup>7</sup> L. G. Efimov,<sup>1</sup> M. Elnimr,<sup>36</sup> J. Engelage,<sup>32</sup> G. Eppley,<sup>37</sup> M. Estienne,<sup>17</sup> L. Eun,<sup>38</sup> O. Evdokimov,<sup>11</sup>  
R. Fatemi,<sup>39</sup> J. Fedorisin,<sup>1</sup> R. G. Fersch,<sup>39</sup> P. Filip,<sup>1</sup> E. Finch,<sup>22</sup> V. Fine,<sup>7</sup> Y. Fisyak,<sup>7</sup> C. A. Gagliardi,<sup>25</sup>  
D. R. Gangadharan,<sup>16</sup> F. Geurts,<sup>37</sup> P. Ghosh,<sup>26</sup> Y. N. Gorbunov,<sup>30</sup> A. Gordon,<sup>7</sup> O. G. Grebenyuk,<sup>3</sup> D. Grosnick,<sup>40</sup>  
S. M. Guertin,<sup>16</sup> A. Gupta,<sup>12</sup> S. Gupta,<sup>12</sup> W. Guryn,<sup>7</sup> B. Haag,<sup>21</sup> O. Hajkova,<sup>14</sup> A. Hamed,<sup>25</sup> L-X. Han,<sup>24</sup>  
J. W. Harris,<sup>22</sup> J. P. Hays-Wehle,<sup>8</sup> M. Heinz,<sup>22</sup> S. Heppelmann,<sup>38</sup> A. Hirsch,<sup>41</sup> E. Hjort,<sup>3</sup> G. W. Hoffmann,<sup>33</sup>  
D. J. Hofman,<sup>11</sup> B. Huang,<sup>27</sup> H. Z. Huang,<sup>16</sup> T. J. Humanic,<sup>6</sup> L. Huo,<sup>25</sup> G. Igo,<sup>16</sup> P. Jacobs,<sup>3</sup> W. W. Jacobs,<sup>42</sup>  
C. Jena,<sup>43</sup> F. Jin,<sup>24</sup> J. Joseph,<sup>5</sup> E. G. Judd,<sup>32</sup> S. Kabana,<sup>17</sup> K. Kang,<sup>29</sup> J. Kapitan,<sup>15</sup> K. Kauder,<sup>11</sup> H. W. Ke,<sup>28</sup>  
D. Keane,<sup>5</sup> A. Kechechyan,<sup>1</sup> D. Kettler,<sup>13</sup> D. P. Kikola,<sup>41</sup> J. Kiryluk,<sup>3</sup> A. Kisiel,<sup>44</sup> V. Kizka,<sup>1</sup> A. G. Knospe,<sup>22</sup>  
D. D. Koetke,<sup>40</sup> T. Kollegger,<sup>45</sup> J. Konzer,<sup>41</sup> I. Koralt,<sup>23</sup> L. Koroleva,<sup>4</sup> W. Korsch,<sup>39</sup> L. Kotchenda,<sup>19</sup> V. Kouchpil,<sup>15</sup>  
P. Kravtsov,<sup>19</sup> K. Krueger,<sup>20</sup> M. Krus,<sup>14</sup> L. Kumar,<sup>5</sup> P. Kurnadi,<sup>16</sup> M. A. C. Lamont,<sup>7</sup> J. M. Landgraf,<sup>7</sup>  
S. LaPointe,<sup>36</sup> J. Lauret,<sup>7</sup> A. Lebedev,<sup>7</sup> R. Lednicky,<sup>1</sup> J. H. Lee,<sup>7</sup> W. Leight,<sup>8</sup> M. J. LeVine,<sup>7</sup> C. Li,<sup>27</sup> L. Li,<sup>33</sup>  
N. Li,<sup>28</sup> W. Li,<sup>24</sup> X. Li,<sup>41</sup> X. Li,<sup>46</sup> Y. Li,<sup>29</sup> Z. M. Li,<sup>28</sup> L. M. Lima,<sup>47</sup> M. A. Lisa,<sup>6</sup> F. Liu,<sup>28</sup> H. Liu,<sup>21</sup> J. Liu,<sup>37</sup>  
T. Ljubicic,<sup>7</sup> W. J. Llope,<sup>37</sup> R. S. Longacre,<sup>7</sup> W. A. Love,<sup>7</sup> Y. Lu,<sup>27</sup> E. V. Lukashov,<sup>19</sup> X. Luo,<sup>27</sup> G. L. Ma,<sup>24</sup>  
Y. G. Ma,<sup>24</sup> D. P. Mahapatra,<sup>43</sup> R. Majka,<sup>22</sup> O. I. Mall,<sup>21</sup> R. Manweiler,<sup>40</sup> S. Margetis,<sup>5</sup> C. Markert,<sup>33</sup> H. Masui,<sup>3</sup>  
H. S. Matis,<sup>3</sup> Yu. A. Matulenko,<sup>34</sup> D. McDonald,<sup>37</sup> T. S. McShane,<sup>30</sup> A. Meschanin,<sup>34</sup> R. Milner,<sup>8</sup>  
N. G. Minaev,<sup>34</sup> S. Mioduszewski,<sup>25</sup> M. K. Mitrovski,<sup>7</sup> Y. Mohammed,<sup>25</sup> B. Mohanty,<sup>26</sup> M. M. Mondal,<sup>26</sup>  
B. Morozov,<sup>4</sup> D. A. Morozov,<sup>34</sup> M. G. Munhoz,<sup>47</sup> M. K. Mustafa,<sup>41</sup> M. Naglis,<sup>3</sup> B. K. Nandi,<sup>9</sup> T. K. Nayak,<sup>26</sup>  
P. K. Netrakanti,<sup>41</sup> L. V. Nogach,<sup>34</sup> S. B. Nurushev,<sup>34</sup> G. Odyniec,<sup>3</sup> A. Ogawa,<sup>7</sup> K. Oh,<sup>31</sup> A. Ohlson,<sup>22</sup>  
V. Okorokov,<sup>19</sup> E. W. Oldag,<sup>33</sup> R. A. N. Oliveira,<sup>47</sup> D. Olson,<sup>3</sup> M. Pachr,<sup>14</sup> B. S. Page,<sup>42</sup> S. K. Pal,<sup>26</sup> Y. Pandit,<sup>5</sup>  
Y. Panebratsev,<sup>1</sup> T. Pawlak,<sup>44</sup> H. Pei,<sup>11</sup> T. Peitzmann,<sup>18</sup> C. Perkins,<sup>32</sup> W. Peryt,<sup>44</sup> P. Pile,<sup>7</sup> M. Planinic,<sup>48</sup>  
M. A. Ploskon,<sup>3</sup> J. Pluta,<sup>44</sup> D. Plyku,<sup>23</sup> N. Poljak,<sup>48</sup> J. Porter,<sup>3</sup> A. M. Poskanzer,<sup>3</sup> B. V. K. S. Potukuchi,<sup>12</sup>  
C. B. Powell,<sup>3</sup> D. Prindle,<sup>13</sup> C. Pruneau,<sup>36</sup> N. K. Pruthi,<sup>2</sup> P. R. Pujahari,<sup>9</sup> J. Putschke,<sup>22</sup> H. Qiu,<sup>49</sup> R. Raniwala,<sup>50</sup>  
S. Raniwala,<sup>50</sup> R. Redwine,<sup>8</sup> R. Reed,<sup>21</sup> H. G. Ritter,<sup>3</sup> J. B. Roberts,<sup>37</sup> O. V. Rogachevskiy,<sup>1</sup> J. L. Romero,<sup>21</sup>  
L. Ruan,<sup>7</sup> J. Rusnak,<sup>15</sup> N. R. Sahoo,<sup>26</sup> I. Sakrejda,<sup>3</sup> S. Salur,<sup>21</sup> J. Sandweiss,<sup>22</sup> E. Sangaline,<sup>21</sup> A. Sarkar,<sup>9</sup>  
J. Schambach,<sup>33</sup> R. P. Scharenberg,<sup>41</sup> A. M. Schmah,<sup>3</sup> N. Schmitz,<sup>51</sup> T. R. Schuster,<sup>45</sup> J. Seele,<sup>8</sup> J. Seger,<sup>30</sup>  
I. Selyuzhenkov,<sup>42</sup> P. Seyboth,<sup>51</sup> N. Shah,<sup>16</sup> E. Shahaliev,<sup>1</sup> M. Shao,<sup>27</sup> M. Sharma,<sup>36</sup> S. S. Shi,<sup>28</sup> Q. Y. Shou,<sup>24</sup>  
E. P. Sichtermann,<sup>3</sup> F. Simon,<sup>51</sup> R. N. Singaraju,<sup>26</sup> M. J. Skoby,<sup>41</sup> N. Smirnov,<sup>22</sup> D. Solanki,<sup>50</sup> P. Sorensen,<sup>7</sup>  
U. G. Souza,<sup>47</sup> H. M. Spinka,<sup>20</sup> B. Srivastava,<sup>41</sup> T. D. S. Stanislaus,<sup>40</sup> D. Staszak,<sup>16</sup> S. G. Steadman,<sup>8</sup>  
J. R. Stevens,<sup>42</sup> R. Stock,<sup>45</sup> M. Strikhanov,<sup>19</sup> B. Stringfellow,<sup>41</sup> A. A. P. Suaide,<sup>47</sup> M. C. Suarez,<sup>11</sup>  
N. L. Subba,<sup>5</sup> M. Sumera,<sup>15</sup> X. M. Sun,<sup>3</sup> Y. Sun,<sup>27</sup> Z. Sun,<sup>49</sup> B. Surrow,<sup>8</sup> D. N. Svirida,<sup>4</sup> T. J. M. Symons,<sup>3</sup>  
A. Szanto de Toledo,<sup>47</sup> J. Takahashi,<sup>35</sup> A. H. Tang,<sup>7</sup> Z. Tang,<sup>27</sup> L. H. Tarini,<sup>36</sup> T. Tarnowsky,<sup>52</sup> D. Thein,<sup>33</sup>  
J. H. Thomas,<sup>3</sup> J. Tian,<sup>24</sup> A. R. Timmins,<sup>10</sup> D. Tlusty,<sup>15</sup> M. Tokarev,<sup>1</sup> S. Trentalange,<sup>16</sup> R. E. Tribble,<sup>25</sup>  
P. Tribedy,<sup>26</sup> O. D. Tsai,<sup>16</sup> T. Ullrich,<sup>7</sup> D. G. Underwood,<sup>20</sup> G. Van Buren,<sup>7</sup> G. van Nieuwenhuizen,<sup>8</sup>  
J. A. Vanfossen, Jr.,<sup>5</sup> R. Varma,<sup>9</sup> G. M. S. Vasconcelos,<sup>35</sup> A. N. Vasiliev,<sup>34</sup> F. Videbæk,<sup>7</sup> Y. P. Vijoyi,<sup>26</sup>  
S. Vokal,<sup>1</sup> S. A. Voloshin,<sup>36</sup> M. Wada,<sup>33</sup> M. Walker,<sup>8</sup> F. Wang,<sup>41</sup> G. Wang,<sup>16</sup> H. Wang,<sup>52</sup> J. S. Wang,<sup>49</sup>  
Q. Wang,<sup>41</sup> X. L. Wang,<sup>27</sup> Y. Wang,<sup>29</sup> G. Webb,<sup>39</sup> J. C. Webb,<sup>7</sup> G. D. Westfall,<sup>52</sup> C. Whitten Jr.,<sup>16</sup> H. Wieman,<sup>3</sup>

1 S. W. Wissink,<sup>42</sup> R. Witt,<sup>53</sup> W. Witzke,<sup>39</sup> Y. F. Wu,<sup>28</sup> Z. Xiao,<sup>29</sup> W. Xie,<sup>41</sup> H. Xu,<sup>49</sup> N. Xu,<sup>3</sup> Q. H. Xu,<sup>46</sup>  
 2 W. Xu,<sup>16</sup> Y. Xu,<sup>27</sup> Z. Xu,<sup>7</sup> L. Xue,<sup>24</sup> Y. Yang,<sup>49</sup> Y. Yang,<sup>28</sup> P. Yepes,<sup>37</sup> K. Yip,<sup>7</sup> I-K. Yoo,<sup>31</sup> M. Zawisza,<sup>44</sup>  
 3 H. Zbroszczyk,<sup>44</sup> W. Zhan,<sup>49</sup> J. B. Zhang,<sup>28</sup> S. Zhang,<sup>24</sup> W. M. Zhang,<sup>5</sup> X. P. Zhang,<sup>29</sup> Y. Zhang,<sup>3</sup> Z. P. Zhang,<sup>27</sup>  
 4 F. Zhao,<sup>16</sup> J. Zhao,<sup>24</sup> C. Zhong,<sup>24</sup> W. Zhou,<sup>46</sup> X. Zhu,<sup>29</sup> Y. H. Zhu,<sup>24</sup> R. Zoukarneev,<sup>1</sup> and Y. Zoukarneeva<sup>1</sup>

5 <sup>1</sup>Joint Institute for Nuclear Research, Dubna, 141 980, Russia

6 <sup>2</sup>Panjab University, Chandigarh 160014, India

7 <sup>3</sup>Lawrence Berkeley National Laboratory, Berkeley, California 94720, USA

8 <sup>4</sup>Alikhanov Institute for Theoretical and Experimental Physics, Moscow, Russia

9 <sup>5</sup>Kent State University, Kent, Ohio 44242, USA

10 <sup>6</sup>Ohio State University, Columbus, Ohio 43210, USA

11 <sup>7</sup>Brookhaven National Laboratory, Upton, New York 11973, USA

12 <sup>8</sup>Massachusetts Institute of Technology, Cambridge, MA 02139-4307, USA

13 <sup>9</sup>Indian Institute of Technology, Mumbai, India

14 <sup>10</sup>University of Houston, Houston, TX, 77204, USA

15 <sup>11</sup>University of Illinois at Chicago, Chicago, Illinois 60607, USA

16 <sup>12</sup>University of Jammu, Jammu 180001, India

17 <sup>13</sup>University of Washington, Seattle, Washington 98195, USA

18 <sup>14</sup>Czech Technical University in Prague, FNSPE, Prague, 115 19, Czech Republic

19 <sup>15</sup>Nuclear Physics Institute AS CR, 250 68 Řež/Prague, Czech Republic

20 <sup>16</sup>University of California, Los Angeles, California 90095, USA

21 <sup>17</sup>SUBATECH, Nantes, France

22 <sup>18</sup>NIKHEF and Utrecht University, Amsterdam, The Netherlands

23 <sup>19</sup>Moscow Engineering Physics Institute, Moscow Russia

24 <sup>20</sup>Argonne National Laboratory, Argonne, Illinois 60439, USA

25 <sup>21</sup>University of California, Davis, California 95616, USA

26 <sup>22</sup>Yale University, New Haven, Connecticut 06520, USA

27 <sup>23</sup>Old Dominion University, Norfolk, VA, 23529, USA

28 <sup>24</sup>Shanghai Institute of Applied Physics, Shanghai 201800, China

29 <sup>25</sup>Texas A&M University, College Station, Texas 77843, USA

30 <sup>26</sup>Variable Energy Cyclotron Centre, Kolkata 700064, India

31 <sup>27</sup>University of Science & Technology of China, Hefei 230026, China

32 <sup>28</sup>Institute of Particle Physics, CCNU (HZNU), Wuhan 430079, China

33 <sup>29</sup>Tsinghua University, Beijing 100084, China

34 <sup>30</sup>Creighton University, Omaha, Nebraska 68178, USA

35 <sup>31</sup>Pusan National University, Pusan, Republic of Korea

36 <sup>32</sup>University of California, Berkeley, California 94720, USA

37 <sup>33</sup>University of Texas, Austin, Texas 78712, USA

38 <sup>34</sup>Institute of High Energy Physics, Protvino, Russia

39 <sup>35</sup>Universidade Estadual de Campinas, Sao Paulo, Brazil

40 <sup>36</sup>Wayne State University, Detroit, Michigan 48201, USA

41 <sup>37</sup>Rice University, Houston, Texas 77251, USA

42 <sup>38</sup>Pennsylvania State University, University Park, Pennsylvania 16802, USA

43 <sup>39</sup>University of Kentucky, Lexington, Kentucky, 40506-0055, USA

44 <sup>40</sup>Valparaiso University, Valparaiso, Indiana 46383, USA

45 <sup>41</sup>Purdue University, West Lafayette, Indiana 47907, USA

46 <sup>42</sup>Indiana University, Bloomington, Indiana 47408, USA

47 <sup>43</sup>Institute of Physics, Bhubaneswar 751005, India

48 <sup>44</sup>Warsaw University of Technology, Warsaw, Poland

49 <sup>45</sup>University of Frankfurt, Frankfurt, Germany

50 <sup>46</sup>Shandong University, Jinan, Shandong 250100, China

51 <sup>47</sup>Universidade de Sao Paulo, Sao Paulo, Brazil

52 <sup>48</sup>University of Zagreb, Zagreb, HR-10002, Croatia

53 <sup>49</sup>Institute of Modern Physics, Lanzhou, China

54 <sup>50</sup>University of Rajasthan, Jaipur 302004, India

55 <sup>51</sup>Max-Planck-Institut für Physik, Munich, Germany

56 <sup>52</sup>Michigan State University, East Lansing, Michigan 48824, USA

57 <sup>53</sup>United States Naval Academy, Annapolis, MD 21402, USA

58 We present first measurements of the evolution of the differential transverse momentum correlation  
 59 function,  $C$ , with collision centrality in Au+Au interactions at  $\sqrt{s_{NN}} = 200$  GeV. This observable  
 60 exhibits a strong dependence on collision centrality that is qualitatively similar to that of number  
 61 correlations previously reported. We use the observed longitudinal broadening of the near-side peak  
 62 of  $C$  with increasing centrality to estimate the ratio of the shear viscosity to entropy density,  $\eta/s$ ,

of the matter formed in central Au+Au interactions. We obtain an upper limit estimate of  $\eta/s$  that suggests that the produced medium has a small viscosity per unit entropy.

PACS numbers: 25.75.Gz, 25.75.Ld, 24.60.Ky, 24.60.-k

Measurements carried out at the Relativistic Heavy Ion Collider (RHIC) during the last decade indicate that a strongly interacting quark gluon plasma (sQGP) is produced in heavy nuclei collisions at very high beam energies [1]. It has emerged that this matter behaves as a “nearly perfect liquid”, i.e., a fluid which has a very small shear viscosity per unit of entropy [1, 2]. It is a fascinating observation that the medium produced in relativistic heavy ion collisions reaches exceedingly large temperatures, of the order of  $2 \times 10^{12}$  K [3], in stark contrast to the very low temperature,  $T < 3$  K, required to achieve superfluid  $^4\text{He}$  [4].

Conclusions concerning the shear viscosity per unit of entropy of the medium produced in Au+Au collisions at RHIC are based largely on comparisons of non-dissipative hydrodynamical calculations of the time evolution of collision systems with measurements of the particle production azimuthal anisotropy characterized by the elliptic flow coefficient  $v_2$  [2, 5]. These calculations describe the  $v_2$  and momentum spectra measured in Au+Au collisions at  $\sqrt{s_{NN}} = 200$  GeV well at midrapidity ( $|\eta| < 1.0$ ), low transverse momentum ( $p_T < 1$  GeV/c), and for mid-central collisions (impact parameter  $b \leq 5$  fm)[1, 5, 6]. A measure of fluidity is provided by the ratio of shear viscosity,  $\eta$ , to entropy density,  $s$ , henceforth referred to as  $\eta/s$ . It has been conjectured that the limit for all relativistic quantum field theories at finite temperature and zero chemical potential is close to the Kovtun-Son-Starinets (KSS) bound,  $\eta/s|_{KSS} = (4\pi)^{-1} \approx 0.08$  [2, 7]. Estimates of  $\eta/s$  based on  $v_2$ , measured in Au+Au collisions at  $\sqrt{s_{NN}} = 200$  GeV, range significantly below the viscosity per unit of entropy ratio of superfluid  $^4\text{He}$  and very close to the quantum limit [2, 5, 8, 9]. Given the importance of viscosity in furthering our understanding of QCD matter, it is of interest to consider alternative measurement techniques to estimate the magnitude of  $\eta/s$ . Measurements of di-hadron correlations in heavy ion collisions, carried out as a function of the relative azimuthal particle emission angle,  $\Delta\phi$ , have greatly advanced the studies of hot and strongly interacting matter at RHIC [10]. Indeed, studies of correlations between low and high  $p_T$  particles have revealed the modification of away-side ( $\Delta\phi \sim \pi$ ) jets and the formation of a longitudinally elongated near-side ( $\Delta\phi \sim 0$ ) structure, known as the ridge, in central Au+Au collisions [11]. Meanwhile, low- $p_T$  di-hadron correlation studies reveal rich correlation structures, particularly on the away-side [11]. However, the interpretation of these different measurements is nontrivial, and a number of competing models invoking different reaction mechanisms have been suggested to explain the data, each with relative success [13]. Thus,

additional observables and measurements are required to discriminate fully among these competing models.

In this work, we present measurements of the differential extension of an integral observable  $C$  [8] in Au+Au collisions at  $\sqrt{s_{NN}} = 200$  GeV. The correlation function  $C$  is defined as follows:

$$C(\Delta\eta, \Delta\phi) = \frac{\left\langle \sum_{i=1}^{n_1} \sum_{j=1, j \neq i}^{n_2} p_{T,i} p_{T,j} \right\rangle}{\langle n \rangle_1 \langle n \rangle_2} - \langle p_T \rangle_1 \langle p_T \rangle_2 \quad (1)$$

where  $\langle p_T \rangle_k \equiv \langle \sum p_{T,i} \rangle_k / \langle n \rangle_k$  is the average momentum, the label  $k$  stands for particles from each event and the brackets represent event ensemble averages.  $\langle n \rangle_k$  is the average number of particles emitted at  $(\eta_k, \phi_k)$ . The indices  $i$  and  $j$  span all particles in a  $(\eta_k, \phi_k)$  bin.  $\Delta\eta = \eta_1 - \eta_2$  and  $\Delta\phi = \phi_1 - \phi_2$  are the relative pseudorapidity and azimuthal angle of measured particle pairs, respectively.

The correlation observable  $C(\Delta\eta, \Delta\phi)$ , defined above, is an extension of the number correlation function  $R_2$  used in various studies [14]. By construction, it measures the degree of correlation between particles emitted at fixed relative pseudorapidity,  $\Delta\eta$ , and azimuthal angle difference,  $\Delta\phi$ , and is as such sensitive to various aspects of the collision dynamics. However, the explicit transverse-momentum weighing provides for additional sensitivity to discriminate and study soft (low  $p_T$ ) vs. hard (high  $p_T$ ) processes. Note that  $C$  differs structurally and quantitatively from the observables  $\langle \delta p_T \delta p_T \rangle$  [15] and  $\Delta\sigma_{p_T}^2$  [16] previously reported by STAR. Differences stem from the fact that  $C$  is sensitive not only to number density fluctuations, but also to  $p_T$  fluctuations, and as such reflects the magnitude of in-medium momentum current correlations [8].

This study is based on an analysis of  $8 \times 10^6$  minimum bias (MB) trigger events recorded by the STAR experiment in the year 2004 (RHIC Run IV). The MB trigger was defined by requiring a coincidence signal of two zero-degree calorimeters (ZDCs) located at  $\pm 18$  m from the center of the STAR Time Projection Chamber (TPC). Data were acquired with forward ( $+z$ -axis) and reverse ( $-z$ -axis) solenoidal magnetic field polarity with nominal field strength of 0.5 T. Collision centrality was estimated based on the uncorrected primary track multiplicity within  $|\eta| < 1.0$ . Nine centrality classes corresponding to 0-5% (most central), 5-10% up to 70-80% (most peripheral) of the total cross-section were used. A mean number of participants,  $N_{part}$ , is attributed to each fraction of the total cross-section using a Glauber Monte Carlo simulation [17].

1 The analysis is restricted to charged-particle tracks  
 2 measured in the TPC with  $|\eta| < 1.0$ . Particles of interest  
 3 for our measurement are those emerging from the bulk of  
 4 the matter. Comparisons of RHIC data to hydrodynamic  
 5 models show that the (near) equilibrium description only  
 6 holds for particles with  $p_T \leq 2$  GeV/ $c$ . For larger mo-  
 7 menta, particle production is dominated by hard pro-  
 8 cesses. Thus, we restrict this measurement to low  $p_T$ , i.e.,  
 9 with both particles in the range  $0.2 < p_T < 2.0$  GeV/ $c$ .  
 10 Tracks were selected on the basis of standard STAR qual-  
 11 ity cuts [18]. To minimize acceptance effects, events were  
 12 analyzed provided their collision vertex lay within a dis-  
 13 tance of  $|z| < 25$  cm from the center of the TPC. How-  
 14 ever, the particle acceptance exhibits a small dependence  
 15 on the collision vertex position, which may introduce ar-  
 16 tificial correlations in the measurement of  $C$ . To avoid  
 17 such effects, we measure  $C$  independently for forward and  
 18 reverse magnetic field settings in 20 vertex- $z$  bins of width  
 19  $\Delta z = 2.5$  cm in the range  $-25 < z < 25$  cm. Then we av-  
 20 erage these measurements to obtain the correlation func-  
 21 tion. Track reconstruction inefficiencies for pairs with  
 22  $\Delta\eta \sim 0$ , due to track crossing or merging in the TPC, are  
 23 corrected for by performing a  $p_T$  and charge sign ordered  
 24 analysis of these pairs. Track pair losses occur when two  
 25 tracks pass nearby one another and produce overlapping  
 26 charge clusters in the TPC. For instance, with a forward  
 27 magnetic field setting (i.e. along the  $+z$ -axis), two posi-  
 28 tive charged particles, with  $p_{T,2} > p_{T,1}$ , may cross in the  
 29 TPC if emitted at pseudorapidity difference  $\Delta\eta \sim 0$ , and  
 30 relative angle  $\Delta\phi < 0$  thereby resulting in pair losses for  
 31  $\Delta\phi < 0$ . Pairs emitted with  $\Delta\phi > 0$  however tend to di-  
 32 verge in the TPC and thus are not subject to such losses.  
 33 In symmetric A+A collisions, pair correlation functions  
 34 are invariant under  $\Delta\phi \rightarrow -\Delta\phi$  reflection. The lost pair  
 35 yield at  $\Delta\phi < 0$  may thus be corrected based on the  
 36 yield at  $-\Delta\phi$ . Same-sign track pairs are recorded with  
 37  $\Delta\phi = -|\Delta\phi|$  for  $p_{T,1} > p_{T,2}$  and  $\Delta\phi = +|\Delta\phi|$  otherwise.  
 38 Pair yields measured for  $-1.0 < \Delta\phi < 0$ , are then substi-  
 39 tuted for those at  $0 < \Delta\phi < 1.0$ , thereby compensating  
 40 for pair losses. A similar technique is used for unlike-sign  
 41 pairs. However, no corrections are made for track pairs  
 42 with  $|\Delta\eta| < 0.032$  and  $|\Delta\phi| < 0.087$  radian (bin at the  
 43 origin). These corrections change the amplitude of  $C$  by  
 44  $< 1\%$  in peripheral collisions and up to 4% in central  
 45 collisions. The measurements of  $C(\Delta\eta, \Delta\phi)$  reported in  
 46 this work were constructed using 31 and 36 bins along  
 47 the  $\Delta\eta$  and  $\Delta\phi$  axes respectively. We verified that the  
 48 results are independent of the bin width.

49 Figure 1 presents the correlation function,  $C$ , for three  
 50 representative collision centralities (a) 70-80%, (b) 30-  
 51 40% and (c) 0-5%. Relative statistical errors range from  
 52 0.8% in peripheral collisions to 0.9% in the most cen-  
 53 tral collisions at the peak of the distribution. Sources  
 54 of systematic errors on the amplitude and shape of the  
 55 correlation function include the collision centrality defi-  
 56 nition on the basis of primary particle multiplicity in the

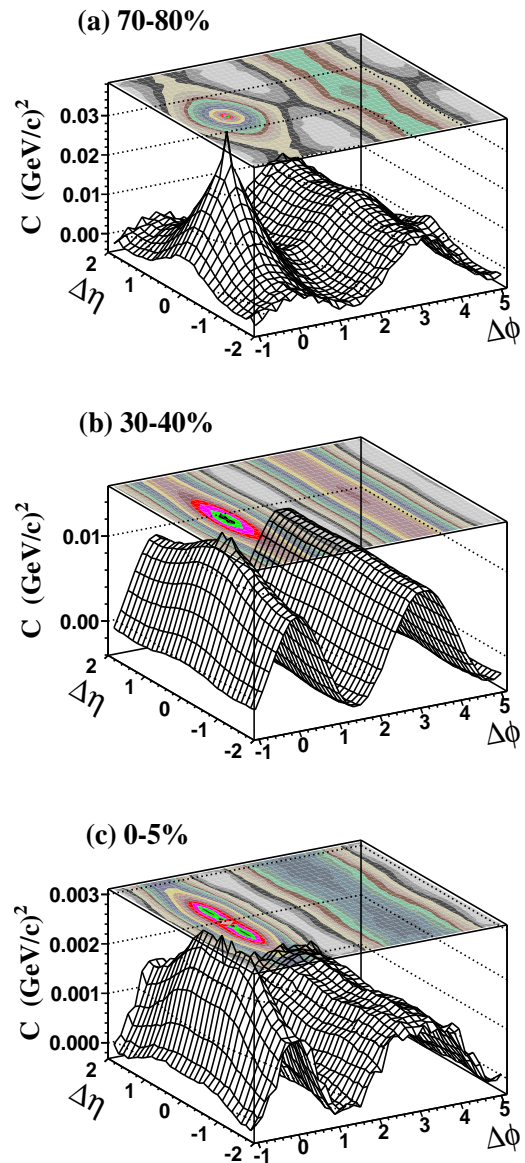


FIG. 1: (Color online) Correlation function,  $C$ , shown for (a) 70-80%, (b) 30-40%, and (c) 0-5% centrality in Au+Au collisions at  $\sqrt{s_{NN}} = 200$  GeV.  $C$  is plotted in units of  $(\text{GeV}/c)^2$ , and the relative azimuthal angle  $\Delta\phi$  in radians.

range  $|\eta| < 1.0$ , finite centrality bin width effects, loss of track reconstruction efficiency at  $p_T < 0.5$  GeV/ $c$ , B-field direction, and high TPC occupancy, as well as contamination of the correlation function from weakly decaying hadrons ( $K_S^0$ ,  $\Lambda$ ), conversion electrons, and HBT correlations. A study of the effect of the centrality definition based on particle multiplicity in the range  $|\eta| < 0.5$ ,  $|\eta| < 0.75$ , and  $|\eta| < 1.0$  compared to that obtained with the ZDC energy reveals that the  $|\eta| < 1.0$  based centrality definition least biases the shape of  $C$  at large  $\Delta\eta$ . Uncertainties on the correlation yield associated with centrality

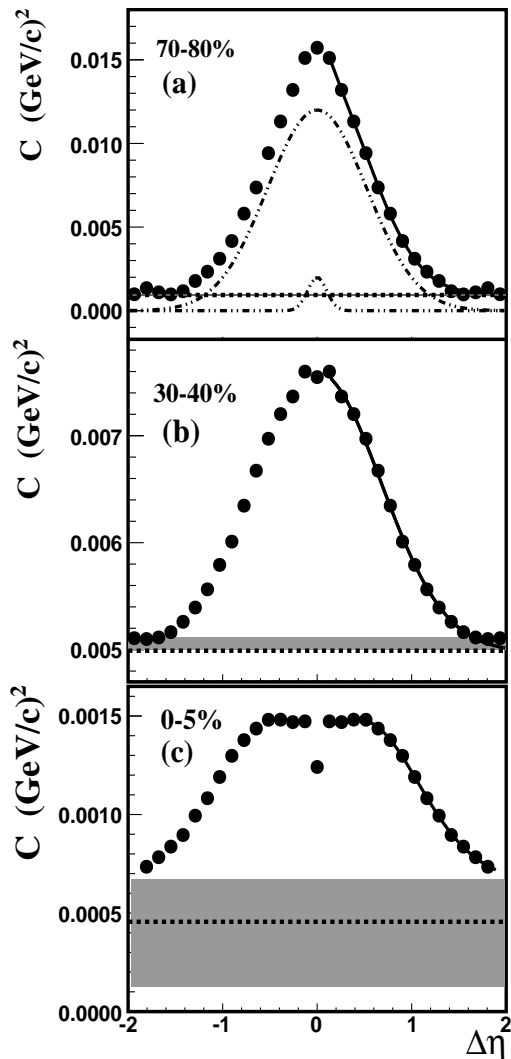


FIG. 2: (a) Projection of the correlation function  $C$ , for  $|\Delta\phi| < 1.0$  radians on the  $\Delta\eta$  axis for 70-80% centrality, (b) 30-40% centrality, and (c) 0-5% centrality in Au+Au collisions at  $\sqrt{s_{NN}} = 200$  GeV. The correlation function  $C$  is plotted in units of  $(\text{GeV}/c)^2$ . The solid line shows the fit obtained with Eq. 2. The dotted line corresponds to the baseline,  $b$ , obtained in the fit and shaded band shows uncertainty in determining  $b$ .

boundaries and bin width vary from 10% in peripheral to less than 1% in the most central collisions. Contamination from weakly decaying particles and conversion electrons is estimated to contribute less than 2% based on measured yields and known material budget of the detector. HBT effects are essentially negligible, due to the large  $p_T$  range used in the measurement.

The overall strength of  $C$  decreases monotonically from peripheral to central collisions. In 70-80% peripheral collisions,  $C$  exhibits a near-side peak centered at  $\Delta\phi \sim \Delta\eta \sim 0$  and a longitudinally extended away-side struc-

ture (i.e., broad in  $\Delta\eta$ ) at  $\Delta\phi \sim \pi$ . This away-side structure largely results from effects associated with momentum conservation [19]. In more central collisions, momentum conservation effects are diluted by increased particle multiplicities, and the near- and away-side observed correlation features may result from a superposition of several mechanisms possibly including resonance and cluster decays, radial flow effects, anisotropic flow effects, initial state fluctuations, and modified jet fragmentation. In mid-central collisions (30-40%), the correlation function exhibits a sizable broadening of the near-side peak and the formation of a near-side ridge-like structure, as well as a strong elliptic flow,  $\cos(2\Delta\phi)$ , modulation [20]. In the most central collisions (0-5%), we observe further longitudinal broadening of the near-side peak while the  $\cos(2\Delta\phi)$  modulation and away-side structures have a much reduced amplitude.

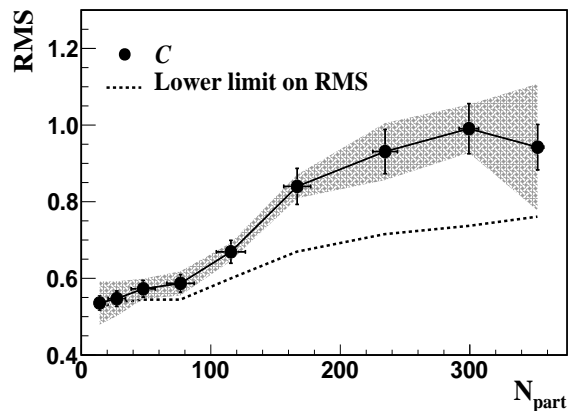


FIG. 3: RMS as function of the number of participating nucleons for the correlation function  $C$ , for nine centrality classes in Au+Au collisions at  $\sqrt{s_{NN}} = 200$  GeV. The dotted line represents a lower limit estimate of the RMS explained in the text and the shaded band represents systematic uncertainties on the RMS.

We next focus on the longitudinal broadening of  $C$  with increasing  $N_{part}$  based on  $\Delta\eta$  projections in the range  $|\Delta\phi| < 1.0$  radians. Figures 2(a-c) show the projections for 70-80%, 30-40%, and 0-5% centralities, respectively. The dip seen at  $\Delta\eta \sim 0$  for 0-5% central collisions (Fig. 2(c)) is a consequence of track merging occurring at  $\Delta\phi \sim \Delta\eta \sim 0$ . We observe that the shape and particularly the width of the projections evolve with collision centrality. We characterize the widths of the distributions by calculating their RMS above a long range baseline,  $b$ , assumed to be constant in the acceptance of our measurement. The baseline,  $b$ , is determined using the following ansatz to fit the projections:

$$g(b, a_w, \sigma_w, a_n, \sigma_n) = b + a_w \exp(-\Delta\eta^2/2\sigma_w^2) + a_n \exp(-\Delta\eta^2/2\sigma_n^2) \quad (2)$$

where  $a_w$  and  $a_n$  stand for the amplitude of wide and

narrow Gaussians with widths  $\sigma_w$  and  $\sigma_n$ , respectively. The offset, narrow Gaussian, wide Gaussian, and full fit are shown in Fig. 2(a) for peripheral collisions. The fits have  $\chi^2$  per degree of freedom values of order unity. The fits are used uniquely for the determination of the offset  $b$ . The amplitudes and widths of the Gaussians are not used in the remainder of this analysis. Uncertainties in the determination of the offset,  $b$ , are shown as dark gray shaded areas in Fig. 2.

Figure 3 shows the RMS of the correlation function as a function of  $N_{part}$ . Vertical lines indicate statistical errors whereas systematic uncertainties on the RMS are indicated by the gray shaded band. Systematic uncertainties arise from several sources. The correlation width exhibits small instrumental dependencies on the magnetic field direction, and the collision vertex position of the order of 3% and 4% respectively in most central collision and much smaller in peripheral collisions. Track merging corrections, discussed above, account for particles losses at  $|\Delta\eta| \sim 0$ ,  $|\Delta\phi| < 1.0$  and lead to negligible,  $\ll 1\%$ , systematic errors on the RMS of the distributions. The correction technique used does not account for losses at  $|\Delta\eta| < 0.032$  and  $|\Delta\phi| < 0.087$  radian (bin at the origin) which are most severe in 0-5% central collisions. This bin is also subject to contamination from  $e^+e^-$  pairs resulting from photon conversions within the apparatus. We estimated the latter two effects introduce small systematic uncertainties,  $< 2\%$ , on the RMS of the correlation functions. The largest source of systematic uncertainties stems from the baseline determination and the lack of knowledge of the correlations long  $\Delta\eta$  range behavior, particularly in central collisions. In order to study these effects, we first estimated a lower bound of RMS values, shown as a dotted line in Fig. 3, by setting the offset equal to the value of the correlation signal at  $\Delta\eta = 2.0$ . This simplistic calculation shows that the RMS exhibits a monotonic growth from peripheral to central collisions. In peripheral collisions, the correlation peak stands atop an approximately flat background but in most central collisions the peak is manifestly broader than the acceptance and this simple estimate is therefore incorrect. We thus used Eq. 2 and systematically studied fits for various number of parameters and fit ranges. Estimated systematic uncertainties on the offset are shown as gray bands in Fig. 2. Uncertainties on the offset and shape of the distribution, particularly in central collisions, lead to systematic uncertainties on the RMS ranging from 10 % in peripheral collisions to 15 % in most central collisions. The above systematic uncertainties are summed in quadrature and shown as a gray shaded band in Fig. 3. The RMS exhibits a modest increase in the range  $N_{part} < 100$  which may in part result from long range multiplicity fluctuations and from incomplete system thermalization achieved in small collision systems. The RMS rises rapidly in the range  $100 < N_{part} < 250$  after which it levels off.

According to [8], shear viscosity should dominate the broadening of the correlation function for sufficiently large and nearly thermalized collision systems. It should thus be possible to utilize the observed broadening to estimate the viscosity of the matter produced in these collisions. However, jets and jet quenching could also in principle contribute to changes in the shape and broadening of the width of the correlation function with varying collision centralities. To examine this possibility, we repeated our analysis in the  $0.2 < p_T < 1.0$  GeV/c and  $0.2 < p_T < 20.0$  GeV/c ranges. Our study shows that particles accepted between  $0.2 < p_T < 20.0$  GeV/c produce essentially identical widths in peripheral collisions. In central collisions, RMS reduces by  $\sim 7\%$  from the RMS widths obtained for the  $p_T$  selection  $0.2 < p_T < 2.0$  GeV/c. However, lowering the upper  $p_T$  cut to 1.0 GeV/c ( $0.2 < p_T < 1.0$  GeV/c) does not change the widths within statistical errors for  $0.2 < p_T < 2.0$  GeV/c range for the most central collisions, and decreases the widths by  $\sim 10\%$  in peripheral collisions. We conclude that broadening effects associated with jets or jet quenching are thus likely limited to less than a 10% effect on the RMS from peripheral to central collisions. We thus proceed to estimate the shear viscosity per entropy of the matter produced in central collisions based on the following formula from Ref. [8].

$$\sigma_c^2 - \sigma_0^2 = 4 \frac{\eta}{T_c s} \left( \tau_0^{-1} - \tau_{c,f}^{-1} \right) \quad (3)$$

where  $\sigma_c$  and  $\sigma_0$  stand for the longitudinal widths of the correlation function in central collisions and at formation time, respectively.  $\tau_0$  refers to the formation time and  $\tau_{c,f}$  is the kinetic freeze-out time at which particles have no further interactions [21].  $T_c$  stands for a characteristic temperature of the system through its evolution, and is here taken to be the critical temperature. We proceed by assuming that viscous broadening dominates the increase in  $C$  with increasing centrality observed in this analysis and utilize Eq. 3 to estimate  $\eta/s$ . We estimate  $\sigma_0 = 0.54 \pm 0.02(stat.) \pm 0.06(sys.)$  by extrapolating the RMS width of  $C$  to  $N_{part} \sim 2$ . The RMS value for most central collisions is  $\sigma_c = 0.94 \pm 0.06(stat.) \pm 0.17(sys.)$ . Using commonly accepted estimates of 1 fm/c, 20 fm/c, and 170 MeV [8] for the formation time, central collision freeze-out, and effective temperature, we obtain a value of  $\eta/s = 0.13 \pm 0.03$ . Inclusion of systematic uncertainties on the widths leads to a range of  $\eta/s = 0.06 - 0.21$ . Figure 4 shows  $\eta/s$  as a function of  $\tau_0^{-1} - \tau_{c,f}^{-1}$  and provides an estimate of theoretical uncertainties based on a literature survey of theoretical estimates for  $\tau_0$  and  $T_c$ .  $\tau_0$  is typically assumed to be in the range 0.6 - 1.0 fm/c (e.g., [8, 21, 22]). Here, we have assumed that the broadening of  $C$  is entirely due to viscous effects. Given that other (unknown) dynamical effects could perhaps also lead to the correlation function broadening, we conclude that our measurement provides an upper limit. Based on the sta-

tistical and systematic uncertainties of our measurement (using one standard deviation) and caveats of the used theoretical model, and using the ranges  $150 < T_c < 190$  MeV and  $0.6 < \tau_0^{-1} - \tau_{c,f}^{-1} < 1.6$  (fm/c) $^{-1}$ , we derive an upper limit of order  $\eta/s \sim 0.3$ .

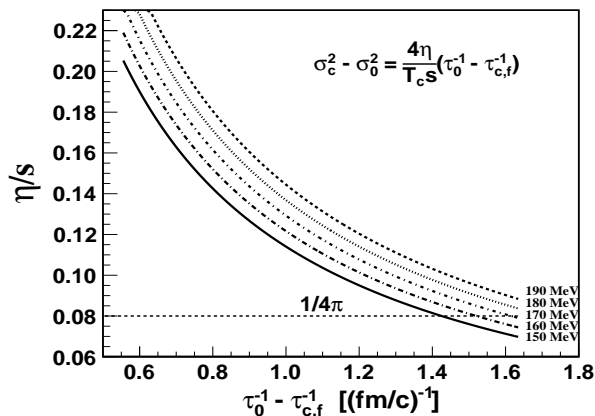


FIG. 4:  $\eta/s$  as a function of  $\tau_0^{-1} - \tau_{c,f}^{-1}$  and  $T_c$ .  $\tau_0$  and  $T_c$  vary from  $0.5 < \tau_0 < 1.5$  fm/c and  $150 < T_c < 190$  MeV, respectively.

In summary, we presented first measurements of the differential transverse momentum correlation function  $C$  from Au+Au collisions at  $\sqrt{s_{NN}} = 200$  GeV. In peripheral collisions,  $C$  has a shape qualitatively similar to that observed in measurements of number density correlations, with a relatively narrow near-side peak near  $\Delta\eta \approx \Delta\varphi \approx 0$  and a longitudinally broad away-side [10, 16]. We find that the near-side peak progressively broadens with increasing number of collision participants while the overall strength of the correlation function decreases monotonically. These results may be used to further constrain particle production and correlation models. We used the observed longitudinal broadening to estimate  $\eta/s$  of the matter formed in central Au+Au collisions. Considering systematic uncertainties in the determination of correlation widths, particularly in central collisions, and assuming somewhat conservative estimates of the temperature, formation and freeze-out times, we obtain a range of  $\eta/s = 0.06 - 0.21$ . This result is remarkably close to the KSS bound,  $(4\pi)^{-1}$ , and is consistent with results obtained from hydrodynamical model comparisons to elliptic flow data [5].

We thank the RHIC Operations Group and RCF at BNL, the NERSC Center at LBNL, and the Open Science Grid consortium for providing resources and support. This work was supported in part by the Offices of NP and HEP within the U.S. DOE Office of Science, the U.S. NSF, the Sloan Foundation, the DFG cluster of excellence ‘Origin and Structure of the Universe’ of Germany, CNRS/IN2P3, STFC and EPSRC of the United Kingdom, FAPESP CNPq of Brazil, Ministry of Ed. and

Sci. of the Russian Federation, NNSFC, CAS, MoST, and MoE of China, GA and MSMT of the Czech Republic, FOM and NWO of the Netherlands, DAE, DST, and CSIR of India, Polish Ministry of Sci. and Higher Ed., Korea Research Foundation, Ministry of Sci., Ed. and Sports of the Rep. Of Croatia, Russian Ministry of Sci. and Tech, and RosAtom of Russia.

- [1] M. Gyulassy and L. McLerran, Nucl. Phys. A **750** (2005) 30.
- [2] R. A. Lacey *et al.*, Phys. Rev. Lett. **98** (2007) 092301; J. L. Nagle, I. G. Bearden and W. A. Zajc, arXiv:1102.0680 [nucl-th]; H. Song and U. W. Heinz, J. Phys. G **36**, 064033 (2009).
- [3] A. Adare *et al.*, [PHENIX Collaboration], Phys. Rev. Lett. **104** (2010) 132301.
- [4] J. G. Dash and R. D. Taylor, Phys. Rev. **99** (1955) 598-599.
- [5] D. Teaney, Phys. Rev. C **68** (2003) 034913; J. Phys. G **30** (2004) S1247.
- [6] P. F. Kolb, P. Huovinen, U. W. Heinz and H. Heiselberg, Phys. Lett. B **500** (2001) 232; P. Huovinen *et al.*, Phys. Lett. B **503** (2001) 58; T. Hirano, Phys. Rev. C **65** (2001) 011901.
- [7] G. Policastro, D. T. Son and A. O. Starinets, Phys. Rev. Lett. **87** (2001) 081601; P. K. Kovtun, D. T. Son and A. O. Starinets, Phys. Rev. Lett. **94** (2005) 111601.
- [8] S. Gavin and M. Abdel-Aziz, Phys. Rev. Lett. **97** (2006) 162302.
- [9] M. Issah and A. Taranenko, [PHENIX Collaboration], arXiv:nucl-ex/0604011; A. Adare *et al.*, [PHENIX Collaboration], Phys. Rev. Lett. **98** (2007) 162301.
- [10] C. Adler *et al.*, [STAR Collaboration], Phys. Rev. Lett. **90** (2003) 082302; J. Adams *et al.*, [STAR Collaboration], Phys. Rev. Lett. **95** (2005) 152301; B. I. Abelev *et al.*, [STAR Collaboration], Phys. Rev. C **80** (2009) 064912; M. M. Aggarwal *et al.*, [STAR Collaboration], Phys. Rev. C **82** (2010) 024912; H. Agakishiev *et al.*, [STAR Collaboration], arXiv:1010.0690 [nucl-ex];
- [11] B. I. Abelev *et al.*, [STAR Collaboration], Phys. Rev. Lett. **102** (2009) 052302.
- [12] H. Agakishiev *et al.*, [STAR Collaboration], accepted for publication in Phys. Rev. C, arXiv:1102.2669v1.
- [13] N. Armesto *et al.*, Phys. Rev. Lett. **93** (2004) 242301; S. A. Voloshin, Phys. Lett. B **632** (2006) 490; M. Strickland *et al.*, Eur. Phys. J. A **29** (2006) 59; A. Majumder *et al.*, Phys. Rev. Lett. **99** (2007) 042301; E. Shuryak, Phys. Rev. C **76** (2007) 047901; A. Dumitru *et al.*, Nucl. Phys. A **810** (2008) 91; C. B. Chiu and R. C. Hwa, Phys. Rev. C **79** (2009) 034901; B. I. Abelev *et al.*, [STAR Collaboration], Phys. Rev. Lett. **103** (2009) 172301.
- [14] See for instance M. Sharma and C. A. Pruneau, Phys. Rev. C **79** (2009) 024905.
- [15] J. Adams *et al.*, [STAR Collaboration], Phys. Rev. C **72** (2005) 044902.
- [16] J. Adams *et al.*, [STAR Collaboration], J. Phys. G **32** (2006) L37.
- [17] J. Adams *et al.*, [STAR Collaboration], Phys. Rev. C **79** (2009) 034909.

- 1 [18] B. I. Abelev *et al.*, [STAR Collaboration], Phys. Rev. C 6  
2 **79** (2009) 024906. 7  
3 [19] N. Borghini, arXiv:0707.0436. 8  
4 [20] D. Teaney, Phys. Rev. C **68** (2003) 034913. 9  
5 [21] J. D. Bjorken, Phys. Rev. D **27** (1983) 140; D. Teaney, 9 [22] H. Song and U. Heinz, Phys. Rev. C **81** (2010) 024905.  
Prog. Part. Nucl. Phys. **62** (2009) 451; K. Dusling *et al.*, Nucl. Phys. A **836** (2010) 159; M. Luzum and P. Romatschke, Phys. Rev. Lett. **103** (2009) 262302.